UILU-ENG 84-3608

Report No. 108

FATIGUE CRACK DEVELOPMENT IN TENSILE-SHEAR SPOT WELDMENTS

by

Gary A. Smith and F. V. Lawrence
Department of Metallurgy and Mining Engineering, UIUC

A Report of the
MATERIALS ENGINEERING - MECHANICAL BEHAVIOR
College of Engineering, University of Illinois at Urbana-Champaign
July 1984

ABSTRACT

This investigation studied fatigue crack initiation and growth in high-strength-low-alloy tensile-shear weldments under R = 0 loading conditions. Specimens were cycled for various percentages of the fatigue life at several load levels, and crack lengths were determined by sectioning and microscopic examination.

Fatigue crack development can be divided into three stages; crack initiation and early growth, through-thickness crack propagation, and crack propagation across the specimen width, each of which accounts for roughly one third of the total fatigue life. Crack initiation and early growth accounts for 50% or more of life if the failure criterion is through-thickness crack penetration. Test results indicate that the sharpness of the weld nugget notch-root radius may be an important factor in fatigue crack development.

ACKNOWLEDGEMENTS

This study was primarily supported by the Fracture Control Program at the University of Illinois. Additional funding was provided by the American Iron & Steel Institute (No. 1201-448) and by the General Motors Corporation.

Professor F. V. Lawrence, Jr., is gratefully acknowledged for his guidance and assistance throughout this investigation. Thanks are extended to K.-M. Ewing and A. F. Houchens of the General Motors Corp. Technical Center for their assistance in preparing the test specimens, and to D. H. Sherman and W. P. Evans of the Caterpillar Tractor Co. Technical Center for performing the residual stress measurements. L. Heubner and F. Lee are also thanked for assisting with the tedious task of polishing the test specimens, as are P. C. Wang and J. C. McMahon for their assistance and for many discussions.

TABLE OF CONTENTS

1. INTRODUCTION

1.1 Recent Trends

Electrical resistance spot welding has been utilized as a joining process in the automotive industry for many years. A schematic of the spot welding process is shown in Fig. 1. The use of spot welds in automobile manufacturing has increased dramatically in recent years, primarily due to the need to reduce automobile weight and increase fuel efficiency. As a result, thinner guages of high-strength-low-alloy (HSLA) steel have replaced thicker, heavier sections of mild steel in many applications. The weight savings obtainable through the implementation of unit-body construction practices have also been realized. Thus, the electrical resistance spot weld has become the principal joining method in use in the automotive industry today; over 4,000 spot welds are used to create a typical automobile. With the continuing trends toward thinner and lighter sheet thicknesses, there is a critical need for a thorough understanding of the fatigue process in electrical resistance spot welds.

1.2 Current Research

The fatigue resistance of tensile-shear spot weldments is influenced by several factors. The geometry of the weldment; i.e., the weld nugget diameter (D), sheet thickness (t), and specimen width (W); the loading history of the welded joint; and the material properties in the base metal and the weld heat affected zone (HAZ) are the most significant factors influencing spot weld fatigue resistance. Davidson (1) has reviewed and summarized the fatigue properties of spot welds and has determined the effect of geometry on the fatigue resistance of tensile-shear spot welds utilizing a fracture mechanics analysis (2).

$$\Delta\sigma = (\sigma_f' - \sigma_o)\cdot(2N_I)^b \tag{3}$$

where $\Delta\sigma$ is the stress amplitude, σ_f' is the fatigue strength coefficient, σ_o is the residual stress at the crack initiation site, $2N_I$ is reversals to fatigue crack initiation, and b is the fatigue strength exponent. The local stress amplitude at the critical region of the weld (the notch-root stress amplitude) can be estimated as $K_{fmax} \cdot \Delta S/2$ so that:

$$K_{fmax} \cdot \Delta S/2 = (\sigma_f' - \sigma_o)\cdot(2N_I)^b \tag{4}$$

where K_{fmax} is the maximum fatigue notch factor and ΔS is the remote stress range.

Microscopic examination of spot welds shows that practically any value of notch-root radius can be observed, and this suggests the existence of a maximum value of K_f for a given weld geometry. This leads to the idea of K_{fmax}, the maximum fatigue notch factor, which is that of the ''worst case'' notch (8) for fatigue crack initiation. K_f can be estimated using Petersen's equation:

$$K_f = 1 + \frac{K_t - 1}{1 + \frac{a}{r}} \tag{5}$$

where K_t is the elastic stress concentration factor (determined as a function of r by finite element methods), (a) is a material parameter, and r is the notch root radius. Differentiating Eq. 5 with respect to (r) leads to a maximum valuc of K_f (K_{fmax}) corresponding to the ''worst case'' notch. Combining the concept of K_{fmax} and Eq. 4 yields

$$\frac{\Delta S}{2} = \frac{(\sigma_f' - \sigma_o)\cdot(2N_I)^b}{K_{fmax}\left[1 + \frac{1+R}{1-R}(2N_I)^b\right]} \tag{6}$$

an expression for the fatigue strength of a spot weld under a given loading condition (R ratio) and cycles to crack initiation (N_I).

The amount of life involved in propagating a fatigue crack to failure (N_P) can be estimated by assuming Paris Power Law crack growth behavior (9):

$$\frac{da}{dN} = C \cdot (\Delta K)^m \tag{7}$$

where C and m are material constants and ΔK is the applied stress intensity range which can be determined experimentally or through finite element methods and which varies strongly with fatigue crack length. Rearranging Eq. 7 and then integrating both sides with respect to N and a, respectively, one can obtain an expression for N_P,

$$N_P = \int_{a_o}^{a_f} \frac{da}{C \cdot (\Delta K)^m} \tag{8}$$

where a_o and a_f are the initial and final crack sizes, respectively. The total life of a spot weld is then estimated by combining the crack initiation life (Eq. 6) and the crack propagation life (results of Eq. 8). Lawrence et al. (6) have observed reasonably good agreement between predicted behavior and experimentally observed fatigue results for spot welds at long lives.

1.3 Scope and Objectives

This study attempts to characterize the fatigue crack initiation and growth process in tensile-shear spot welds. The scope and objectives of this study were:

1. To study quantitatively fatigue crack initiation and growth behavior in tensile-shear spot welds at several load levels.
2. To evaluate and modify, if necessary, the I-P model with respect to the fatigue crack behavior observed during this study.

2. EXPERIMENTAL PROCEDURES

2.1 Specimen Material and Geometry

The material used in this study was a hot-rolled galvanized high-strength-low-alloy (HSLA) sheet steel (Inland Steel Hi-Form 60®) which has a minimum yield strength of 60 ksi. (414 MPa). The published cyclic fatigue properties (10) are as shown in Table 1. The material sheet thickness was 0.055-in. including the galvanized coating. This steel contains 0.07% carbon, niobium and cerium additions, and is similar to SAE 960X. The nominal chemical composition is tabulated in Table 2. The specimens were of the tensile-shear goemetry with dimensions as shown in Fig. 3.

2.2 Welding Conditions

The specimens were prepared at the General Motors Corporation Technical Center. The spot welds were produced with a single-phase, microprocessor-controlled AC electrical resistance spot welding unit. The nominal welding current (RMS value of the secondary current) was 12.7 kiloamperes and was monitored with a torroidal pick-up located around the lower electrode. The nominal welding time was 20 cycles, and the nominal electrode force (monitored with a hydraulic force gauge) was 825 lbs. (3.67 kN). Size 2, A-Nose Cap Type electrodes (RWMA Class II material) were used for welding. The electrode caps were conditioned by preparing 100 spot welds on excess sheet stock before proceeding to weld the test specimens. The complete welding proccdurcs are shown in Table 3.

2.3 Testing Procedures

The test program was as follows. First, a series of tests were conducted to develop an S-N curve. Then, four load levels were selected, corresponding to various fatigue lives. The specimens were thus divided into four groups, one group for each load level. The selected load levels and corresponding fatigue lives are shown in Table 4. Specimens were then cycled for various percentages of the fatigue life (i.e., 10%, 25%, 35%,...) at each load level. The S-N curve is shown in Fig. 4, along with the number of cycles to which each of the sectioned specimens was subjected.

The testing was conducted in the Materials Engineering Research Laboratory at the University of Illinois. The weldments were fatigue tested in ''MTS'' computer-controlled test machines, and the specimens were gripped with shims to avoid the introduction of bending stresses during testing. The testing conditions were load control, 0-max-0 load cycle (R=0), and test frequencies of from 4 to 50 Hz.

2.4 Crack Length Determination

After testing, the weld nugget was sectioned parallel to the loading axis, through the sheet thickness, off-center. A diagram of the sectioning method is shown in Fig. 5. A low-speed metallographic diamond saw was used for sectioning to minimize smearing of the fatigue cracks, and the sectioned weld nugget was mounted in epoxy resin to facilitate metallographic examination. The specimen was then mechanically polished using standard metallographic techniques, chemically milled (with a solution consisting of 85 ml of 30% H_2O_2, 15 ml of H_2O, and 5 ml of 48% HF) to remove any smearing imparted by polishing, and examined with a Zeiss metallograph. Polaroid photographs of the weld nugget and associated

fatigue cracks were taken, and crack lengths were measured from the photographs. The specimen was then repolished mechanically, removing approximately 0.002-in. of the weld nugget, and the measurement procedure was repeated. Thus a profile of fatigue crack length as a function of position through the nugget was obtained. This data was converted to polar coordinates to yield crack length data as a function of angle around the weld nugget. This procedure was repeated for each specimen, so that the fatigue crack length was obtained as a function of both testing cycles and percentage of life for each load level.

At first, the accurate determination of maximum crack length required sectioning the specimens 15 to 20 times per specimen. Later, as it became apparent that the maximum crack length invariably occurred near the centerline of the weld nugget, fewer sections were required; and as a result, most specimens were sectioned 5 to 10 times. One exception will be discussed subsequently.

3. TEST RESULTS

3.1 Fatigue Crack Length

The centerline of the weld nugget for each specimen was determined to be the location of the maximum nugget width observed during the sectioning process. The nugget centerline was then taken as $\theta = 0°$. The maximum observed crack length invariably occurred at or near the observed weld nugget center.

Fatigue cracks generally developed at both the top and bottom portions of the weld nugget, with one usually being longer than the other. This crack was referred to as the primary crack, while the shorter crack was referenced as the secondary crack (Fig. 5). The fatigue crack length data for the four groups of specimens are presented in Tables 5 through 8. The samples with crack lengths given as ''specimen separation'' were tested until failure. These data were used to develop the initial S-N curve.

The fatigue crack length vs. test cycles data are plotted in Figs. 6 through 9. The open circles represent the primary cracks and the closed circles the secondary cracks. The average life to failure for each particular load level is noted on each graph. The dotted line is an exponential power law ''least-squares'' fit to the data. The fit was calculated by utilizing all of the primary and secondary crack length data for cracks which were greater than 0.005-in. in length. This lower cut-off was selected primarily because of the fact that for small cracks in a tensile-shear spot weldment, the crack experiences both Mode I and Mode II type crack opening behavior, the exact nature of which is not well understood.

3.2 Fatigue Crack Shape

The fatigue cracks that were observed in this study generally propagated at an angle of $60° < \phi < 80°$ from the original line of fusion of the weld nugget. Finite element analyses by Ho (6) of tensile-shear specimens similar to those used in this study indicate the principal stress distribution at the notch-root reaches a maximum value at $\phi \sim 73°$ (Fig. 10). This range of angles is also consistent with calculations by Pook. Other finite element analyses by Ho (6) show that the principal stress distribution around the weld nugget remains near the maximum value for $\theta \sim \pm 60$ from the loading axis (Fig. 11).

One specimen was exhaustively studied and provides additional information concerning the shape of the developing fatigue crack(s). This specimen was tested for 300,000 cycles, corresponding to 42% of the average fatigue life (721,900 cycles) at the test load of 500 lbs. (2.22 kN). The specimen was then sectioned, as was previously described. However, rather than simply sectioning the sample until the nugget center and associated maximum crack lengths were observed and then stopping, sectioning was continued until the fatigue cracks had disappeared completely, which procedure required sectioning this specimen 39 times. The data obtained during this excercise are plotted in Fig. 12, along with semi-elliptical crack shapes which were estimated from the crack length data. From this figure, it appears that multiple fatigue crack initiation is occurring in tensile-shear geometry spot weldments at the load levels studied, as would be expected on the basis of the analyses performed by Ho (6). These analyses suggest that the principle stresses around the weld nugget do not significantly diminish over the range of angles for which fatigue cracks were observed in these specimens.

4. DISCUSSION

4.1 Partitioning of Life

The crack length data presented in Figs. 6 through 9 indicate the existence of three distinct regions of fatigue crack growth behavior. These regions will be denoted as Stage I, Stage II, and Stage III, respectively. Stage I is thought to consist of fatigue crack initiation and early growth behavior. This is the period of total life devoted to the initiation of a fatigue crack at the notch-root of a spot weld and its growth to a length of 0.01-in. The period of total life involved in the propagation of a fagigue crack through the sheet thickness until it reaches the specimen surface will be considered to be Stage II. Stage III is defined as being the period of total life necessary to grow a crack transverse to the sheet thickness until specimen separation occurs. The relative portions of total life devoted to Stages I, II, and III type fatigue crack growth are shown in Fig. 13. These stages of fatigue crack growth will be dealt with in greater detail below.

4.2 Crack Initiation and Early Growth (Stage I)

The total fatigue life (N_T) of a weldment can be defined as the number of cycles required to cause specimen separation. However, an alternative criterion for failure is the number of cycles (N'_T) necessary for the initiation and subsequent growth of a fatigue crack through the sheet thickness (Stage I and Stage II behavior only). The data in Fig. 13 show that, if the former failure criterion (N_T) is utilized, up to 30% of the total fatigue life of a tensile-shear spot weldment is involved in the initiation of a crack at the notch-root of the weld nugget and subsequent growth of this crack to a length of 0.01-in. If, however, the alternative failure criterion (N'_T) is utilized, 50% or more of the fatigue life of a

tensile-shear spot weldment is involved in crack initiation and early growth behavior, as is shown in Fig. 14. The use of this criterion for failure is desirable because it characterizes the fatigue behavior of the spot weld nugget itself; whereas the use of the former criterion for failure results in a greater dependence of weldment fatigue life upon specimen width, due to the period of life involved in Stage III crack growth. It is evident from Figs. 13 and 14 that crack initiation and early growth is an important phenomenon in the fatigue behavior of tensile-shear spot weldments at the load levels selected for this study.

One of the most important factors affecting fatigue crack initiation and early growth in tensile-shear spot welds is the sharpness of the notch-root radius of the weld nugget. The stress intensity at and near the notch increases greatly as the root radius of the notch decreases, and the fatigue life decreases accordingly. Both Pook (7) and Wang (11) have developed analytical expressions relating the effective initial stress intensity to the notch-root radius at the weld nugget. However, the value of the notch-root radius can vary greatly for a single weld nugget, as is shown in Fig. 15, in which the photographs of the primary and secondary cracks developed during the testing of specimen B4 are shown. The primary crack (Fig. 15a) was 0.0448-in. in length, and initiated due to the high stress concentration present at the sharp notch-root radius. The secondary crack (Fig. 15b) initiated and grew under the influence of the lower stress intensity associated with the larger root radius at this portion of the notch, and was thus only 0.0148-in. in length. This behavior was observed in all specimens where significant differences in notch-root radii were discernable.

Multiple fatigue crack initiation was discussed in Section 3.2 (Fig. 12). Multiple fatigue cracks were frequently observed during sectioning of

the specimens, and were present in specimens tested at each of the four load levels. Figure 16 contains both bright-field and dark-field photomicrographs of the multiple cracks which were observed during the sectioning of specimen B3. The location of these cracks is that of the primary crack shown in Fig. 5, and their appearance is similar to that of the multiple cracks observed in specimens tested at other load levels.

Previous work by Wojnowski (12) attempted to characterize fatigue crack initiation using radiography to determine fatigue crack length. This method was not successful, due to the limited resolution of the x-rays in measuring the total crack length which resulted in erroneously short measurements of fatigue crack lengths.

4.3 Stage II Crack Propagation

Stage II fatigue crack behavior involves the period of total life spent propagating a crack of 0.01-in. initial length through the sheet thickness until it reaches the specimen surface. This behavior may include up to 30% of the fatigue life of a test specimen. If the alternative failure criterion (N'_T) discussed earlier is utilized, Stage II behavior accounts for up to 50% of the fatigue life of the weld nugget.

This region of crack growth may be characterized by the Paris Power Law (9), Eq. 7. Since crack length (a) is known as a function of cycles (N) for the four test groups (Figs. 6 through 9), da/dN can be determined by taking the derivative of the ''best-fit'' curves through the data. If C and m are also known, the calculation of the stress intensity range (ΔK) is straightforward. The values of C and m which were utilized were those published for a ferritic-pearlitic steel (13):

$C = 3.6 \times 10^{-10}$ $\quad ksi.\sqrt{in}$

$m = 3.0$

The stress intensity range as a function of crack length was then determined for each of the four load levels used in this study.

Since the value of ΔK depends on the applied load range (ΔP), $\Delta K/\Delta P$ rather than ΔK is plotted as a function of crack length in Fig. 17, as are the initial $\Delta K/\Delta P$ values (plotted at a = 0-in.) which were determined by Pook (7) and by Wang's finite element analysis (denoted FEM) (11). The initial stress intensity ranges (ΔK_i) calculated by Pook and Wang are in reasonable agreement with each other (30% difference). It is also apparent from Fig. 17 that the effective stress intensity increases by at least a factor of 2 as the crack grows through the specimen sheet thickness. The four curves are quite similar qualitatively, but it is also apparent that ΔK is a more complex function of ΔP than was estimated by simply using $\Delta K/\Delta P$. If this relationship between ΔK and ΔP were known, the ΔK versus a curves for the four load levels should reduce to a single curve. It is thought that weld nugget rotation (discussed earlier), which varies greatly with applied load range ΔP has a strong effect on ΔK.

4.4 Stage III Crack Propagation

Stage III fatigue crack behavior is the period of total life during which the fatigue crack propagates transverse to the sheet width until specimen separation occurs. This stage can involve up to 60% of the fatigue life of the test specimen at the loal levels studied. It can be seen from Fig. 13 that the percentage of life involved in Stage III behavior increases with increasing life which suggests that the stress intensity threshold for non-propagating cracks is being approached.

4.5 Other Observations

Fatigue cracks were observed developing at the surface of the specimens tested at load levels corresponding to total lives of 2.6 and 9.7 million cycles. These cracks initiated near the shoulder of the indentations formed by the welding electrodes, and their growth was perpendicular to the applied load direction. These cracks were most likely a result of the residual stresses present at the surface of the weld nugget. Residual stresses were measured at the Caterpillar Tractor Co. Technical Center and were found to be 60 ksi. (414 MPa) in tension, which is at or near the yield strength of the material. These residual stresses would likely be relieved during the first few test cycles of the low cycle (high stress) test groups and indeed surface cracks were not observed in specimens tested at the higher load levels. Surface cracks were never observed to grow to a significant length or to link up with a weld nugget initiated crack. The presence of these cracks may have increased the scatter in the data at long lives, but any other effect is probably negligible.

There are some indications that the observed variations in weld nugget notch-root radius, and associated fatigue crack behavior, may be influenced by expulsion. Expulsion is caused by excessive heating during the welding cycle and is generally thought to have an adverse effect on spot weld fartigue resistance. However, work by Lawrence et al. (3) and by Kimchi (14) has shown little effect of expulsion on spot weld fatigue behavior. In addition, radiography of several specimens during the course of this study has indicated a relationship between the location of the expelled material and nugget notch-root radius. Specimens were radiographed prior to testing, and if expulsion was indicated, the expelled region of the weld nugget was noted. After testing and subsequent sectioning, the locations

of large nugget notch-root radii were found to correspond to the regions where expulsion was indicated by radiography. However, the data available is insufficient to establish a direct relationship.

4.6 Suggestions for Future Studies

A study similar to this, conducted under R = -1 loading conditions, would be of interest, as would be a study conducted under a variable loading history, which is thought to simulate spot weld service conditions. Determination of the relationship between nugget notch-root radii and weld expulsion would also be valuable, as would be the analytical determination of the relationship between stress intensity (ΔK) and applied load (ΔP).

5. CONCLUSIONS

1. Crack initiation and early growth is an important factor in the fatigue resistance of tensile-shear spot weldments at the load levels studied (R = 0 conditions), where crack initiation and early growth accounts for up to 30% of the total fatigue life (N_T) of the specimen. Initiation and early growth account for 50% or more of the lifetime if failure is defined as crack penetration through the sheet thickness (N'_T).

2. Fatigue crack behavior in tensile-shear spot weldments can be separated into three distinct regions: Stage I, fatigue crack initiation and early growth; Stage II, crack penetration through the sheet thickness; and Stage III, crack growth across the specimen width.

3. Stage III crack growth, across the specimen width, accounts for 60% of the total specimen life at $N_T \sim 10^7$ cycles, and appears to be increasing with decreasing load levels. This suggests that the effective stress intensity is approaching the threshold for non-propagating cracks.

4. Weld nugget notch-root radius appears to be an important factor in the fatigue behavior of tensile-shear spot weldments.

Table 1

Yield Strength and Cyclic Fatigue Parameters
of Galvanized SAE 960X

Property	Symbol	SI Units	English Units
Yield Strength	σ_y	424 MPa	61.5 ksi
Fatigue Strength Coefficient	σ'_f	553 MPa	80.2 ksi
Fatigue Strength Exponent	b	-0.054	-0.054
Fatigue Ductility Coefficient	ε'_f	1.893	1.893
Fatigue Ductility Exponent	c	-0.798	-0.798
Strength Coefficient	K'	531 MPa	77.0 ksi
Work Hardening Exponent	n'	0.068	0.068

Table 2

Nominal Chemical Composition
of Galvanized SAE 960X

C(%)	Mn(%)	P(%)	S(%)	Si(%)	Nb(%)	Al(%)	Ce(%)
0.07	0.06	0.11	0.016	0.02	0.029	0.08	0.026

Table 3

Welding Procedures

Electrode Force Pounds (kN)	Hold Time (Cycles)	Weld Time (Cycles)	Weld Current (kAmps)
825(3.67)	30	20	12.7

Table 4

Load Ranges and Associated Fatigue Lives

Load Range lbs.(kN)	Average Fatigue Life (Cycles)
800 (3.56)	108,700
500 (2.22)	721,900
400 (1.78)	2,598,700
350 (1.56)	9,747,300

Table 5

Test Results for Specimens Subjected to
800 lbs. (3.56 kN) Load Range

Test Cycles ($x10^3$)	Percent of Life*	Test Frequency (Hz)	Maximum Primary Crack Length (inches)	Maximum Secondary Crack Length (inches)
5	5	5	0.0011	0.
10	9	10	0.0023	0.0006
15	14	4	0.0100	0.0030
15	14	10	0.0077	0.0004
20	18	4	0.0043	0.0026
25	23	4	0.0066	0.0050
30	28	9	0.0084	0.0031
40	37	30	0.0602†	0.0192
50	46	30	0.0434	0.0049
60	55	30	0.0448	0.0079
95	100	10	Specimen	Separation
117	100	10	Specimen	Separation
115	100	50	Specimen	Separation

* Average Life - 108,700 Cycles
† Fatigue Crack Through Sheet Thickness

Table 6

Test Results for Specimens Subjected to
500 lbs. (2.22 kN) Load Range

Test Cycles ($x10^3$)	Percent of Life*	Test Frequency (Hz)	Maximum Primary Crack Length (inches)	Maximum Secondary Crack Length (inches)
50	7	10	0.0033	0.
100	14	10	0.0045	0.0013
180	25	30	0.0148	0.0090
200	27	10	0.0254	0.0053
253	35	30	0.0463	0.0164
300	42	9	0.0128	0.0087
325	45	30	0.0291	0.0042
400	55	9	0.0551†	0.0527†
500	69	5	0.0529†	0.0528†
705	100	10	Specimen	Separation
721	100	10	Specimen	Separation
741	100	10	Specimen	Separation

* Average Life = 721,900 Cycles
† Fatigue Crack Through Sheet Thickness

Table 7

Test Results for Specimens Subjected to
400 lbs. (1.78 kN) Load Range

Test Cycles ($x10^3$)	Percent of Life*	Test Frequency (Hz)	Maximum Primary Crack Length (inches)	Maximum Secondary Crack Length (inches)
205	8	30	0.0060	0.
390	15	50	0.0011	0.
500	19	30	0.0255	0.
650	25	50	0.0061	0.
820	32	30	0.0240	0.
1,128	43	30	0.0476	0.
1,500	58	50	0.0033	0.0010
994	100	30	Specimen	Separation
2,389	100	30	Specimen	Separation
3,100	100	30	Specimen	Separation
3,110	100	50	Specimen	Separation
3,400	100	50	Specimen	Separation

* Average Life = 2,598,700 Cycles

Table 8

Test Results for Specimens Subjected to
350 lbs. (1.56 kN) Load Range

Test Cycles ($x10^3$)	Percent of Life*	Test Frequency (Hz)	Maximum Primary Crack Length (inches)	Maximum Secondary Crack Length (inches)
1,000	10	25	0.0025	0.
2,500	26	25	0.0115	0.
3,500	36	25	0.0515†	0.
5,000	51	50	0.0006	0.
4,299	100	50	Specimen	Separation
6,381	100	25	Specimen	Separation
9,218	100	50	Specimen	Separation
9,527	100	50	Specimen	Separation
19,311	100	50	Specimen	Separation

* Average Life = 9,747,300 Cycles
† Fatigue Crack Through Sheet Thickness

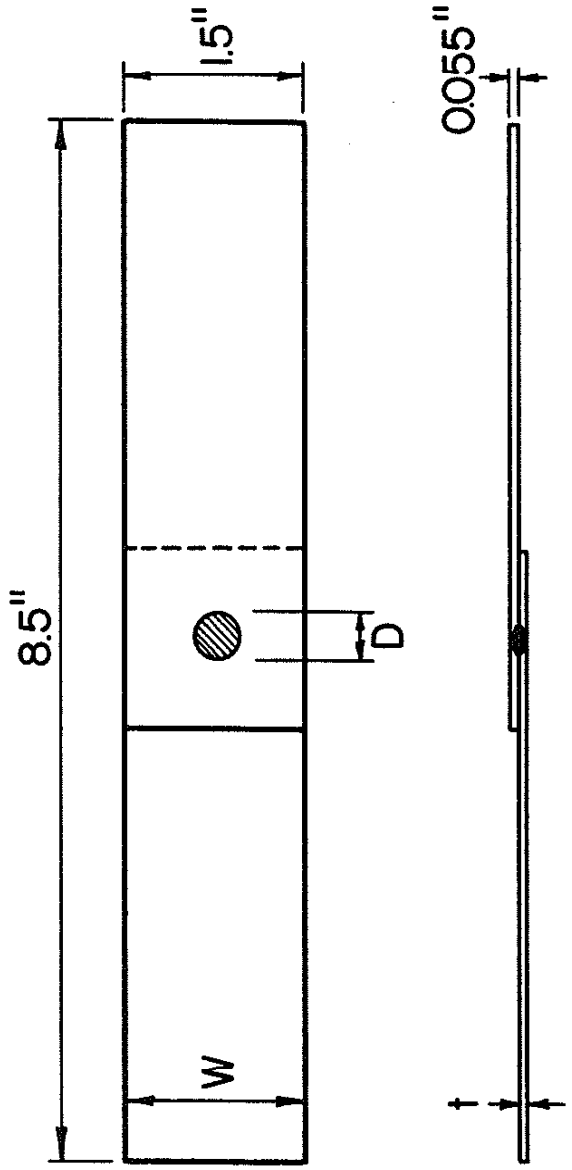

Fig. 3. Dimensions of the Tensile-Shear Test Specimen.

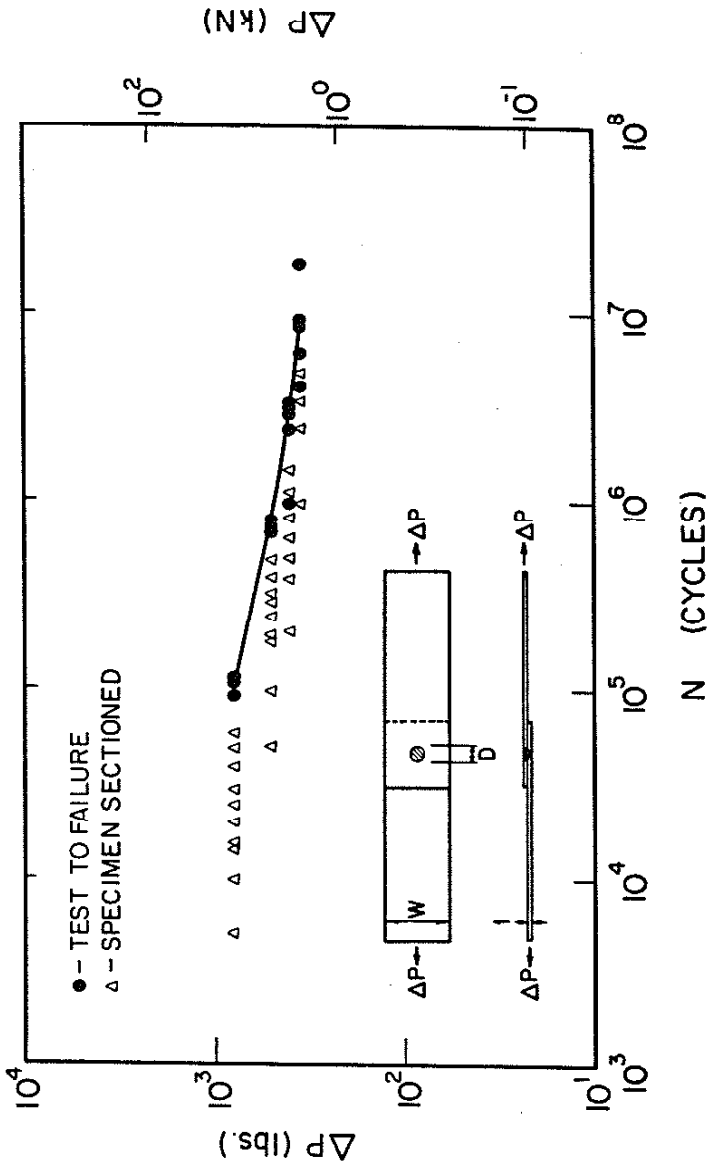

Fig. 4. S-N Curve Showing Relationship Between Test Specimens.

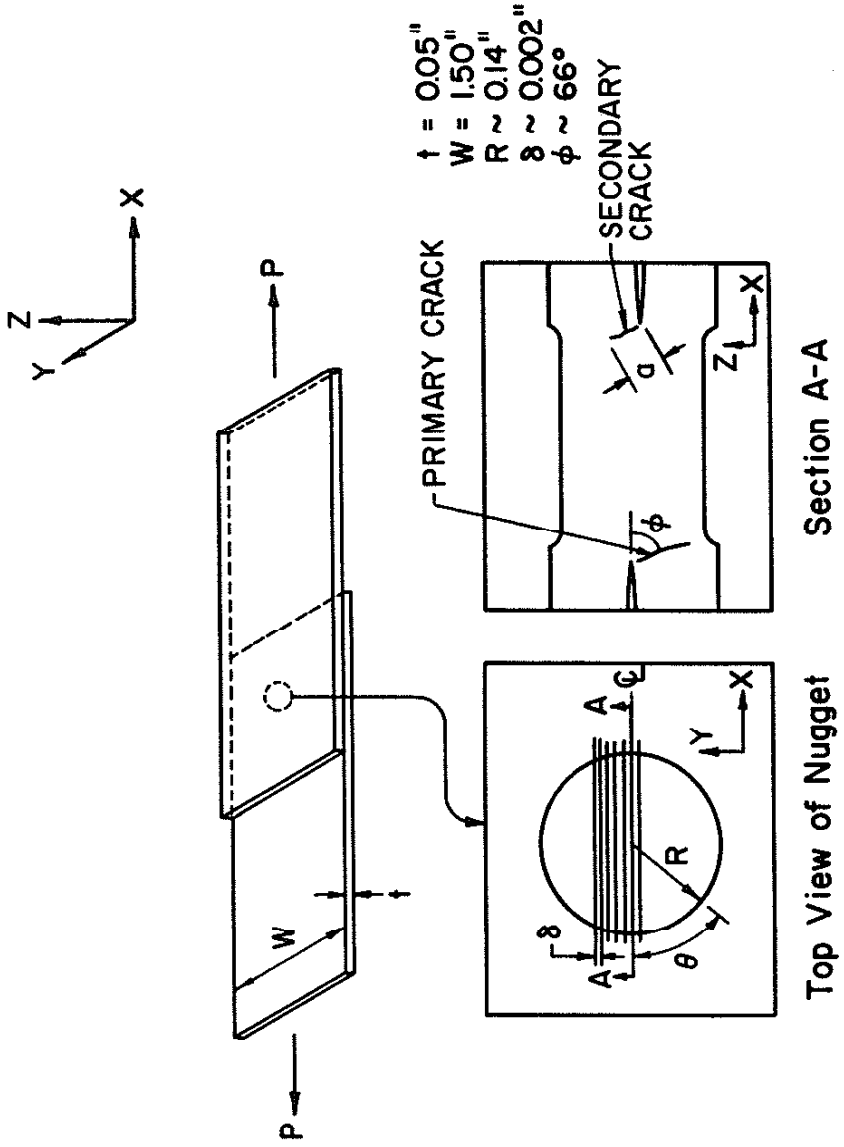

Fig. 5. Sectioning Method and Crack Locations.

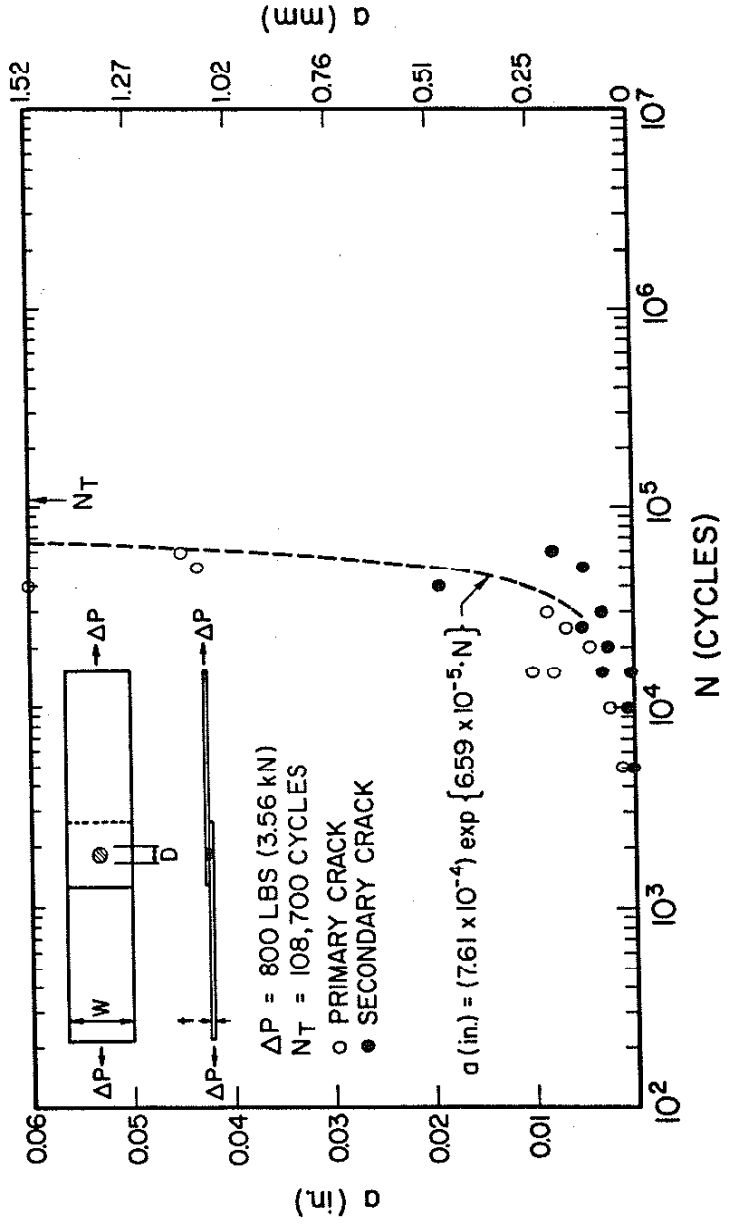

Fig. 6. Fatigue Crack Length vs. Test Cycles for Specimens Subjected to 800 lbs. Load.

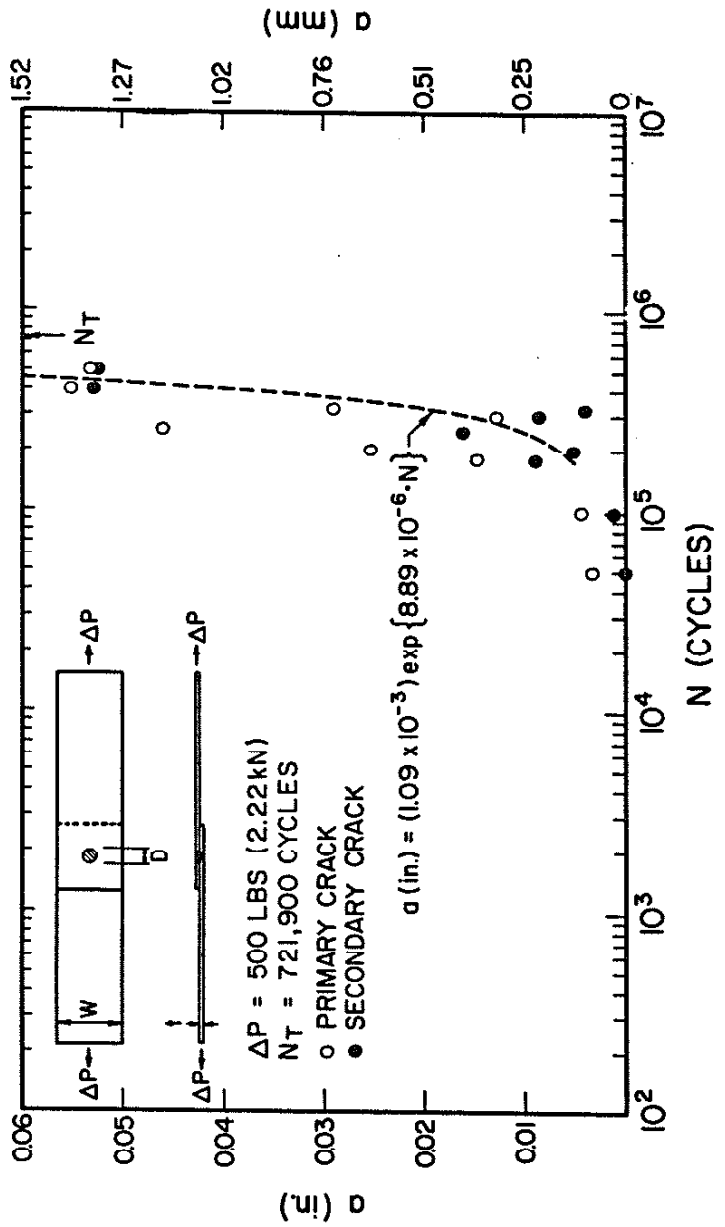

Fig. 7. Fatigue Crack Length vs. Test Cycles for Specimens Subjected to 500 lbs. Load.

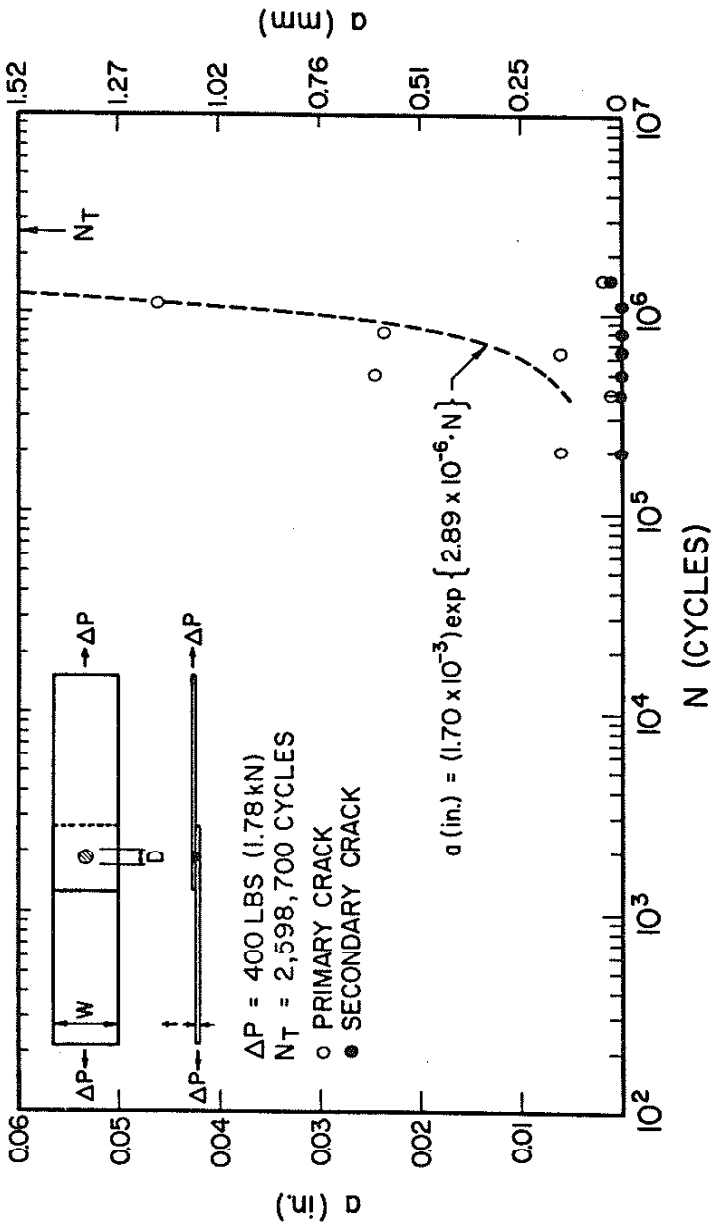

Fig. 8. Fatigue Crack Length vs. Test Cycles for Specimens Subjected to 400 lbs. Load.

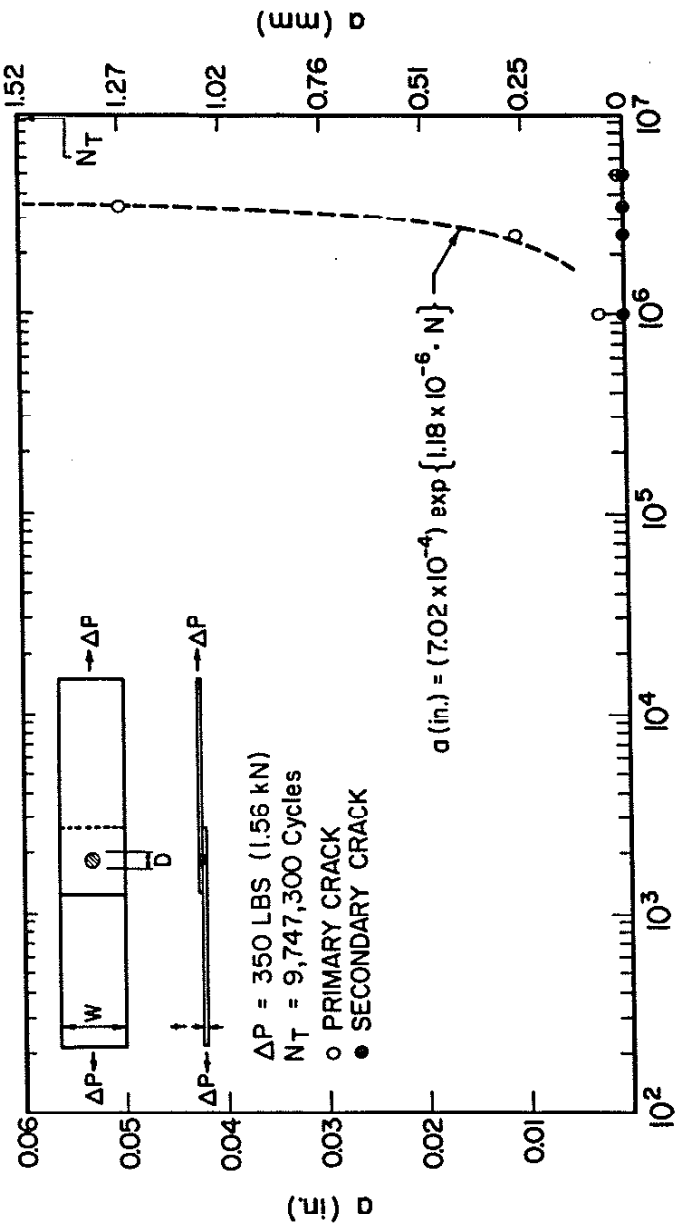

Fig. 9. Fatigue Crack Length vs. Test Cycles for Specimens Subjected to 350 lbs. Load.

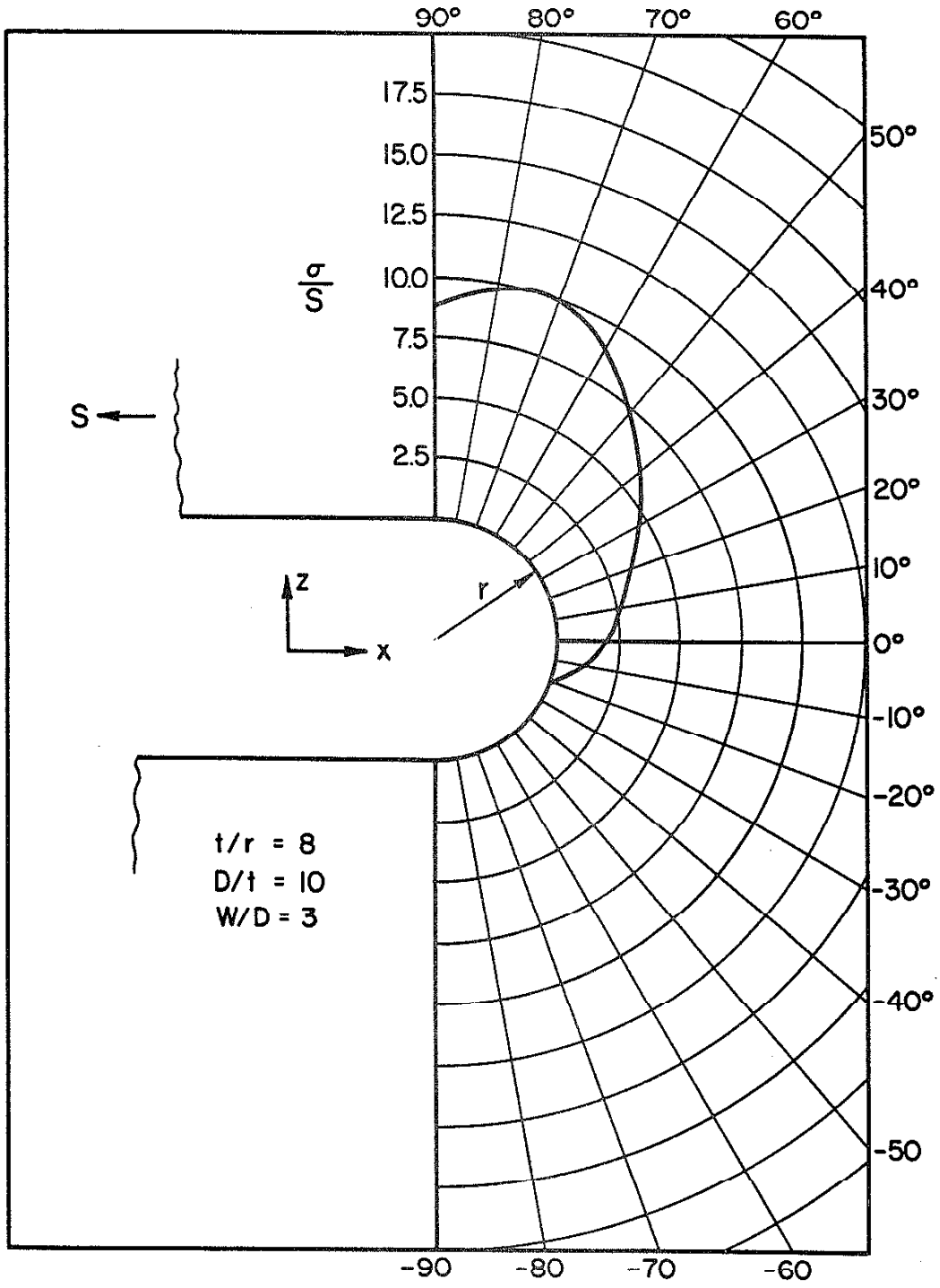

Fig. 10. Principal Stress Distribution at the Notch Root.

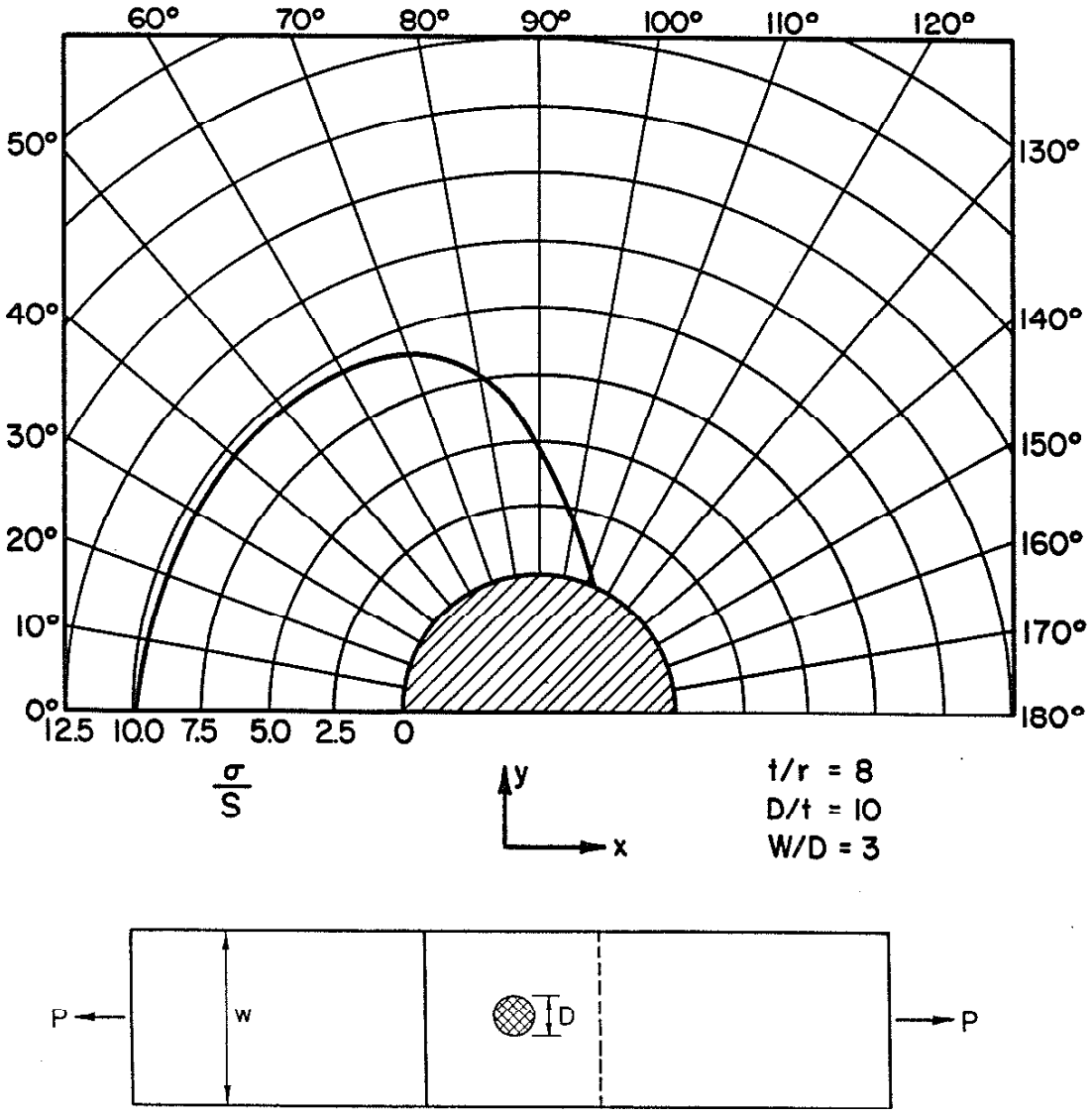

Fig. 11. Principal Stress Distribution Around the Nugget Circumference.

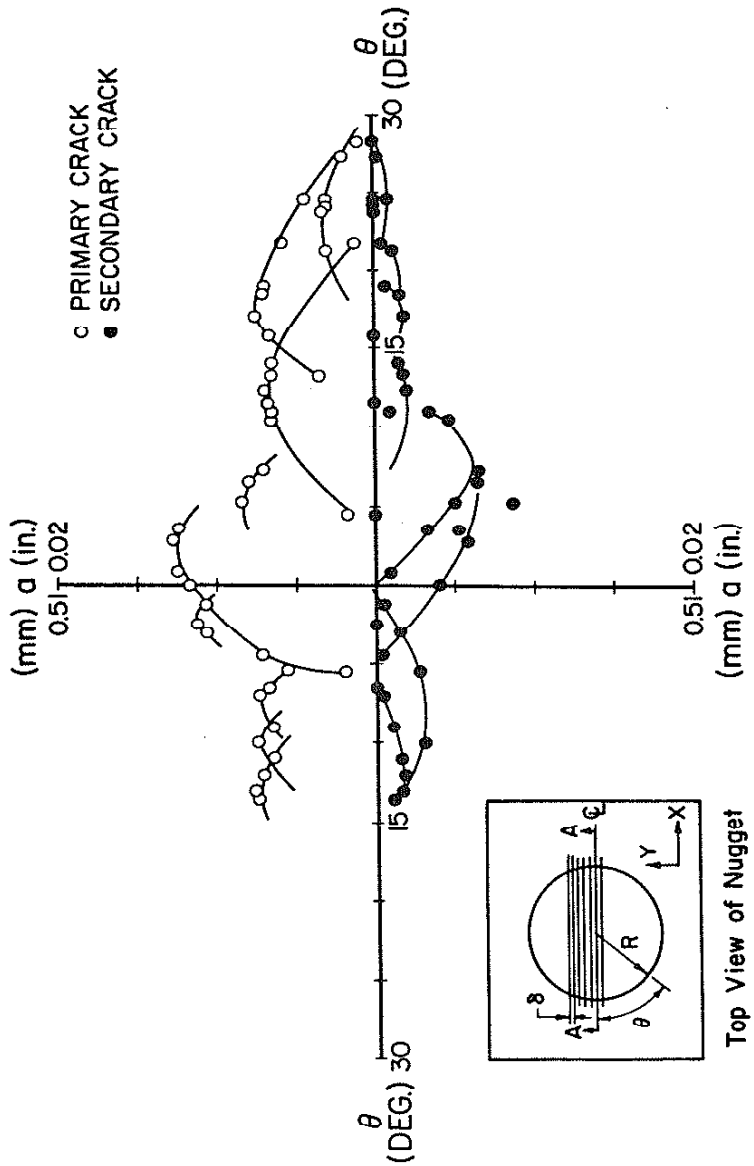

Fig. 12. Fatigue Crack Length vs. θ for Specimen Subjected to 300,000 Cycles at 500 lbs. Load.

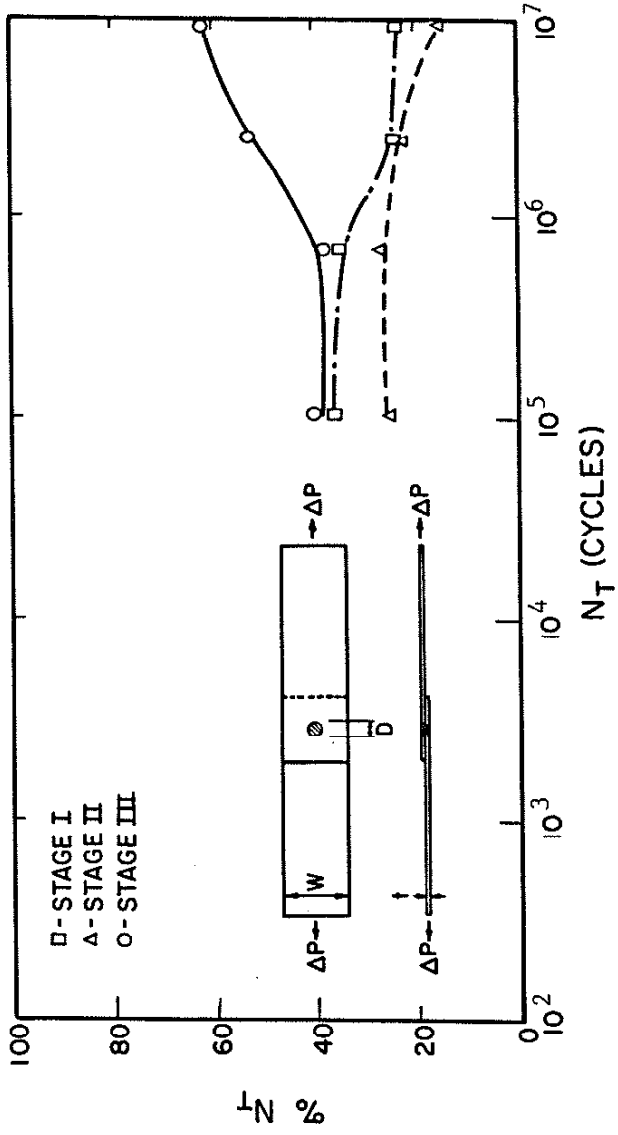

Fig. 13. Percent of Life per Stage vs. Total Life.

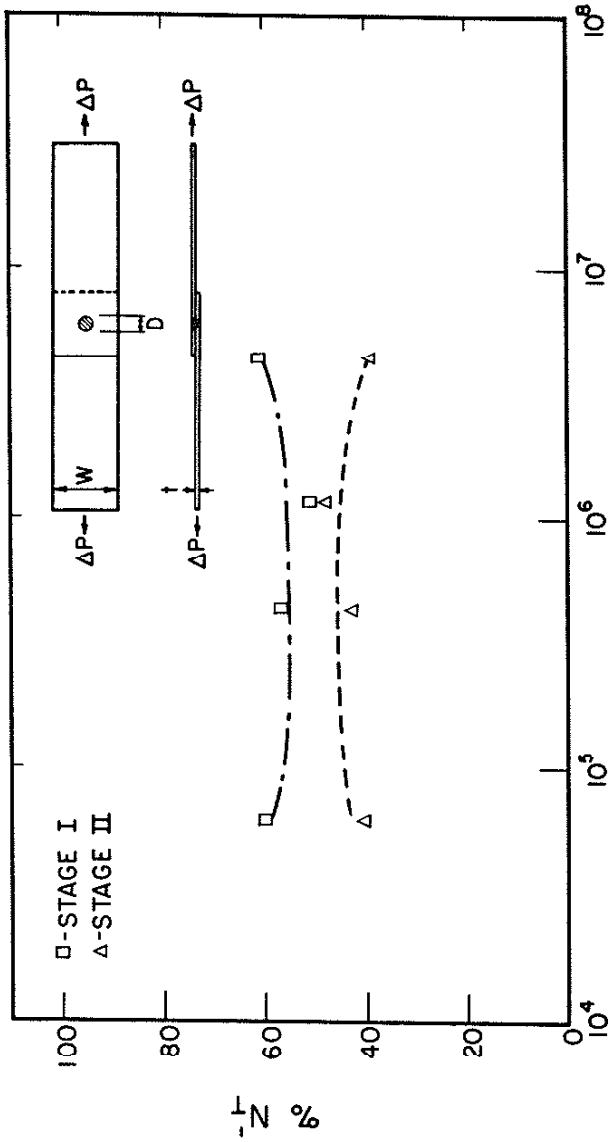

Fig. 14. Percent of Life per Stage vs. Life to Surface Crack (N_T').

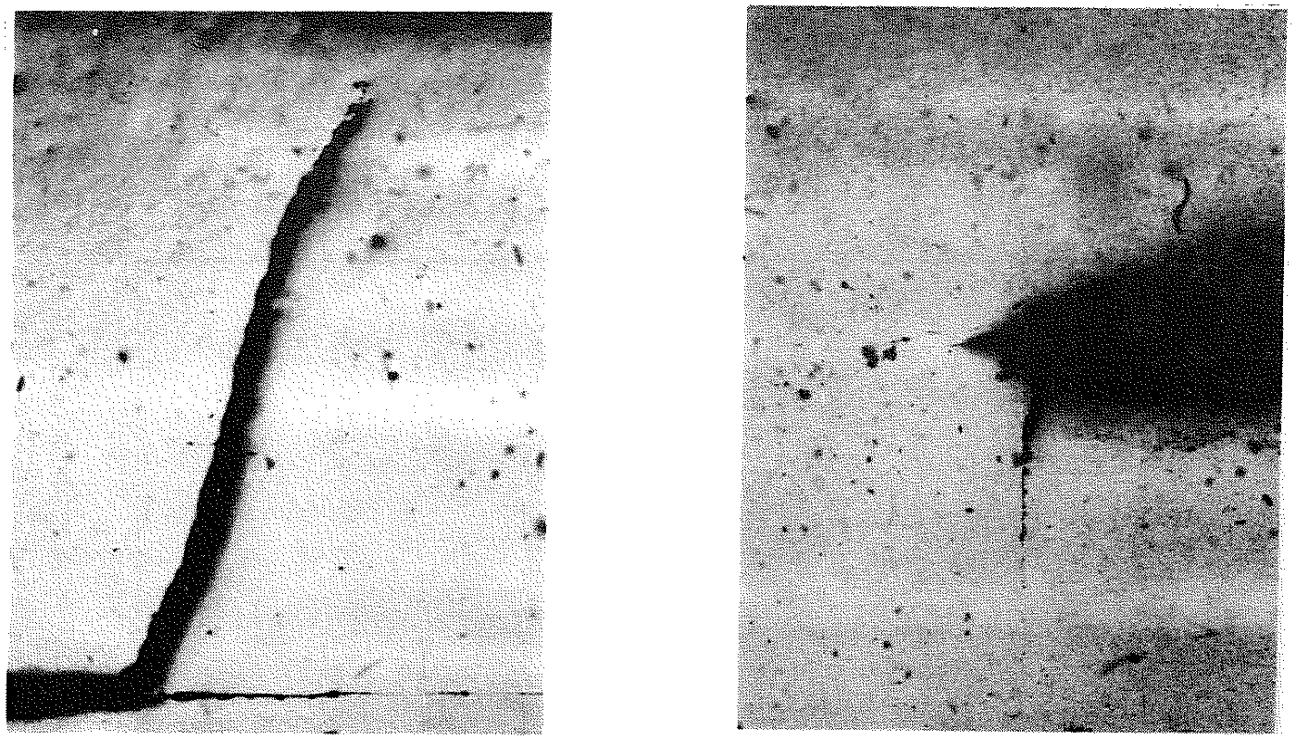

(a) (b)

Fig. 15. Notch Root Radii and Associated Fatigue Cracks Observed During Sectioning of a Single Spot Weld (78x magnification).

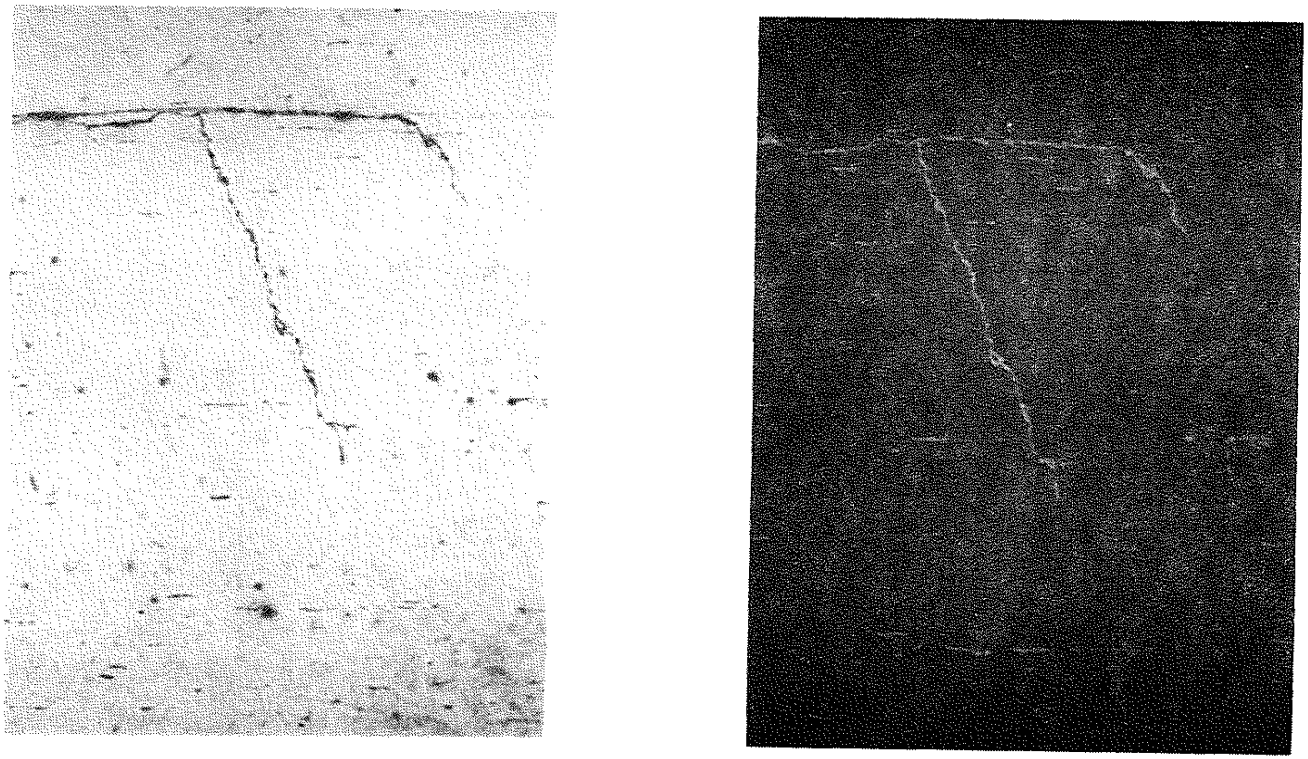

(bright-field) (dark-field)

Fig. 16. Multiple Cracks Observed in Specimen B3 (191x magnification).

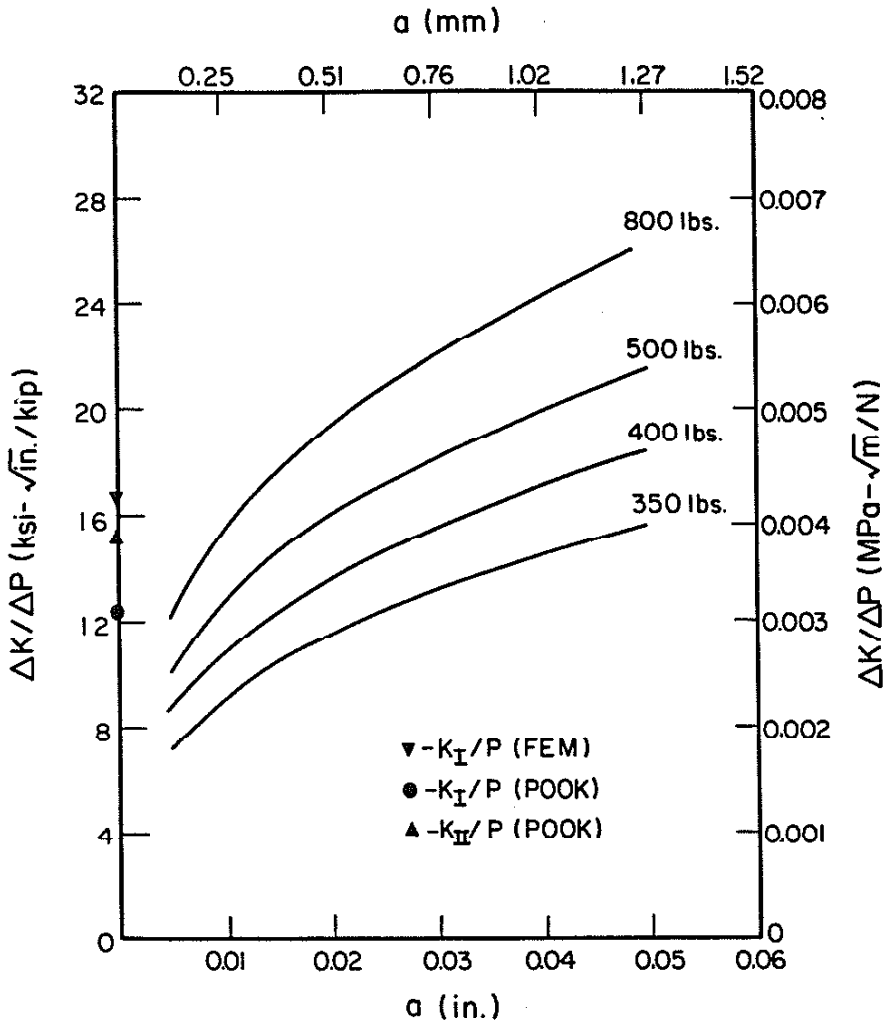

Fig. 17. Stress Intensity/Load vs. Crack Length for the Test Load Levels.

REFERENCES

1. Davidson, J. A. "A Review of the Fatigue Properties of Spot Welded Sheet Steels," paper 830033 presented at the 1983 SAE International Congress and Exposition, Detroit, Michigan, February 1983.

2. Davidson, J. A., and E. J. Imhof, Jr. "A Fracture Mechanics and System Stiffness Approach to Fatigue Performance of Spot Welded Sheet Steels," paper 830034 presented at the 1983 SAE International Congress and Exposition, Detroit, Michigan, February 1983.

3. Lawrence, F. V., Jr., P. C. Wang, and H. T. Corten. Unpublished research for General Motors Corporation, 1983.

4. Matsoukas, G., G. P. Steven, and Y. W. Mai. "Fatigue of Spot Welded Lap Joints," International Journal of Fatigue, Vol. 6, No. 1, January 1984.

5. Davidson, J. A., and E. J. Imhof, Jr. "The Effect of Tensile Strength on the Fatigue Life of Spot Welded Sheet Steels," paper 840110 presented at the SAE International Congress and Exposition, Detroit, Michigan, February 1984.

6. Lawrence, F. V., Jr., P. C. Wang, N.-J. Ho, and H. T. Corten. "Estimating the Fatigue Resistance of Tensile-Shear Spot Welds," Fracture Control Program Report No. 48, University of Illinois, March 1983.

7. Pook, L. P. "Approximate Stress Intensity Factors for Spot and Similar Welds," National Engineering Laboratory Report No. 588, April 1975.

8. Hudak, S. K., Jr., O. H. Burnside, and K. S. Chan. "Analysis of Corrosion Fatigue Crack Growth in Welded Tubular Joints," to be presented at the Offshore Technology Conference, Houston, Texas, May 1984.

9. Paris, P. C., and F. Erdogan. "A Critical Analysis of Crack Propagation Laws," Transactions of the ASME, J. of Basic Engineering, Series D, Vol. 85, 1963.

10. Bhat, S. P. "Prediction of Thickness Reductions from Fatigue Properties of High Strength Steels," SAE Technical Paper No. 840010, 1984.

11. Wang, P. C. Private communication.

12. Wojnowski, D. A. "Fatigue Fracture in Tensile-Shear Spot Weldments," M.S. Thesis, University of Illinois, 1983.

13. Socie, D. F., M. R. Mitchell, and E. M. Caulfield. "Fundamentals of Modern Fatigue Analysis," Fracture Control Program Report No. 26, University of Illinois, revised January 1978.

14. Kimchi, M. "Spot Weld Properties when Welding with Expulsion-A Comparative Study," presented at the American Welding Society Convention, Philadelphia, Pennsylvania, April 1983.